Chinese Journal of
POLYMER SCIENCE

ARTICLE

https://doi.org/10.1007/s10118-021-2634-8
Chinese J. Polym. Sci. **2021**, *39*, 1634–1644

High Performance Electrospun Polynaphthalimide Nanofibrous Membranes with Excellent Resistance to Chemically Harsh Conditions

Meng-Jie Yuan[a], Zhao-Yu Hu[a], Hong Fang[a], Shu-Jing Li[b], Hong-Tao Guo[b], Ru-Bei Hu[b], Shao-Hua Jiang[b,c*], Kun-Ming Liu[d], and Hao-Qing Hou[a*]

[a] *Department of Chemistry and Chemical Engineering, Jiangxi Normal University, Nanchang 330022, China*
[b] *Jiangsu Co-Innovation Center of Efficient Processing and Utilization of Forest Resources, International Innovation Center for Forest Chemicals and Materials, College of Materials Science and Engineering, Nanjing Forestry University, Nanjing 210037, China*
[c] *Shandong Key Laboratory of Biochemical Analysis; College of Chemistry and Molecular Engineering, Qingdao University of Science and Technology, Qingdao 266042, China*
[d] *Faculty of Materials Metallurgy and Chemistry, Jiangxi University of Science and Technology, Ganzhou 341000, China*

Abstract Polynaphthalimide (PNI) with six-membered imide ring ($_6$-PI) has better chemical resistance than five-membered imide ring ($_5$-PI), but is difficult to be processed into nanofibers due to the poor processability. In this work, we proposed a template strategy to fabricate nanofiber $_6$-PI membranes and their composite membranes. Neat $_6$-PI and $_6$-PI composite fibrous membranes were prepared using high-molecular-weight polymers $_5$-PAA and PVP as templates by electrospinning. FTIR, DMA, TGA and tensile tests were used to characterize their chemical structures, thermal stability and mechanical properties. Further eye-observation, micro-morphology investigation and tensile tests were applied to evaluate the chemical resistance of nanofibrous membranes in strong acid, strong alkaline, and concentrated salt. The results demonstrated that $_6$-PI nanofibrous membranes possessed the best thermal stability, best acid, alkaline, and salt resistance with the highest mechanical retention. This study will provide basic information for high-performance electrospun $_6$-PI nanofiber membranes and provide opportunities for applications of PIs in different chemically harsh environments.

Keywords Polynaphthalimide; Nanofibrous membrane; Strong acid; Strong base; Salt

Citation: Yuan, M. J.; Hu, Z. Y.; Fang, H.; Li, S. J.; Guo, H. T.; Hu, R. B.; Jiang, S. H.; Liu, K. M.; Hou, H. Q. High performance electrospun polynaphthalimide nanofibrous membranes with excellent resistance to chemically harsh conditions. *Chinese J. Polym. Sci.* **2021**, *39*, 1634–1644.

INTRODUCTION

Electrospun nanofibrous membranes possess many advantages of small fiber diameter, high porosity, large specific surface area, high surface energy, large aspect ratio, and easy-tailed functions.[1–5] Therefore, electrospun nanofibrous membranes have been extensively applied in many fields.[6–21] However, their further applications in harsh environments are greatly limited due to the types of polymers. Therefore, it is highly required to develop high-performance electrospun fibrous membranes with excellent mechanical properties, thermal stability, and chemical resistance for harsh environment applications.[22] Among different polymers, polyimides (PIs) possess superior mechanical properties and thermal stabilities because of their special molecular structures.[23–26] In general, PI nanofibrous membranes could be easily fabricated by electrospinning from their precursor, poly(amic acid) (PAA), followed by thermal imidization. Electrospun PI nanofibrous membranes possess both the advantages of nanofibrous membranes and PIs, and have been broadly applied in fiber reinforced composites,[23,24] battery separators,[27,28] thermal insulation,[29,30] proton exchange membranes,[31] liquid filtration,[32] high-temperature filtration,[33] protective clothes,[34] *etc.*

Although electrospun PI nanofibrous membranes possess various remarkable advantages and show widespread applications, their poor hydrolysis resistance especially alkaline hydrolysis resistance seriously limits their broader applications.[35,36] It is well known that there are two five-membered imide rings in the main chain of PI molecules. Such imide groups are sensitive to humid acidic or alkaline environment. Especially the PI molecular chains would be degraded rapidly in alkaline due to the OH^- induced hydrolysis.[37–39] To improve the acidic and alkaline hydrolysis resistance of PI materials, researchers have reported some valuable studies. Tao *et al.* prepared soluble fluorinated polybenzimidazopyrrolones from monomers of fluorine-containing tetramine and dianhydride.[40] The prepared polybenzimidazopyrrolones membranes showed excellent alkaline hydrolysis resistance. However, on the one hand, this sort of polypyrrole did not belong to the PI materials; on the other hand, the fluorine-containing monomer is too expensive, which limits its practical

* Corresponding authors, E-mail: shaohua.jiang@njfu.edu.cn (S.H.J.)
E-mail: haoqing@jxnu.edu.cn (H.Q.H.)

Received June 4, 2021; Accepted July 30, 2021; Published online September 6, 2021

applications. The easy hydrolysis of normal PI ($_5$-PI) could be attributed to the planar five-membered imide ring, which possesses high bond angle tension and low structural stability. Therefore, use a special dianhydride monomer, such as naphthalenetetracarboxylic dianhydride, to react with diamine to form a PI with a six-membered imide ring structure ($_6$-PI), which could improve the acid and alkali resistance of the PI materials, and makes this polynaphthalimide (PNI) with better stability to hydrolysis.[41–43] Although there are still countable reports regarding the investigation of PNI resistance to acid or alkaline, PNI proton exchange membrane from naphthalene tetraformic acid dianhydride and diamine containing sulfonic acid group have been reported,[44] suggesting the good resistance of PNI to chemicals. However, because of the weaker reaction activity of six-membered dianhydride than that of five-membered dianhydride, it is difficult to obtain high molecular weight precursor polymers of PNI in aprotic polar solvent at room temperature.[45,46] Generally, low molecular weight six-membered PI ($_6$-PI) could be synthesized directly by one-pot high temperature reaction with *m*-cresol as solvent, benzoic acid as catalyst,[47] and isoquinoline as dehydrating agent.[48,49] On the one hand, *m*-cresol solvent possesses high toxicity and volatility at a high temperature, which is not beneficial for industrialization development and application; on the other hand, the low molecular weight also limits their application of $_6$-PI as fibrous membranes because of their weak mechanical properties.

To address the weak mechanical properties of $_6$-PI fibers because of the low molecular weight of their precursor, poly(naphthalenamic acid) ($_6$-PAA), in this work, a template strategy (sacrifice template method and composite template method) combined with electrospinning technique is adopted to produce a series of $_5$-PI and $_6$-PI nanofibrous membranes for resistance evaluation to chemically harsh conditions, such as strong acid, strong alkaline, and concentrated salt. In detail, during the polycondensation process, a strong nucleophilic acylation catalyst, 4-(*N*,*N*-dimethylamino) pyridine (DMAP), is added to give rise to the $_6$-PAA oligomers with molecular weight as high as possible. After that, the $_6$-PAA oligomers are blended with poly(vinyl pyrrolidone) (PVP) or high molecular weight (five-membered ring) PAA ($_5$-PAA) to prepare $_6$-PAA/PVP or $_6$-PAA/$_5$-PAA composite nanofibrous membranes by electrospinning. After imidization at different temperatures, $_6$-PI/PVP, neat $_6$-PI and $_6$-PI/$_5$-PI nanofibrous composite membranes are obtained for chemical resistance tests. The corresponding chemical resistances are evaluated by the eye-observation, micro-morphology investigation and tensile tests.

EXPERIMENTAL

Materials

4,4'-Oxydianiline (ODA, analytically pure, Changzhou Sunlight Pharmaceutical Co., Ltd., China) and 3,3',4,4'-biphenyltetracarboxylic dianhydride (BPDA, analytically pure, Changzhou Sunlight Pharmaceutical Co., Ltd., China) are purified by sublimation before use. 1,4,5,8-Naphthalenetetracarboxylic dianhydride (NTDA, analytically pure, Zhengzhou alpha Chemical Co., Ltd., China) is dried under vacuum at 200 °C for 6 h. 4-Dimethylaminopyridine (DMAP, Shanghai Aladdin Biochemical Technology Co., Ltd., China) and poly(vinyl pyrrolidone) (PVP, Yingbike New Materials Technology Co., Ltd., Shanghai, China, M_w: 1.76×10^6) were used as received. *N*,*N*-dimethylacetamide (DMAc, analytically pure, Nanjing Teling Tianamine Fine Chemical Co., Ltd., China) and dimethyl sulfoxide (DMSO, analytically pure, Nanjing Teling Tianamine Fine Chemical Co., Ltd., China) were purified by A4 molecular sieve.

Preparation of $_6$-PI, $_6$-PI/PVP and $_6$-PI/$_5$-PI Nanofibrous Membranes

ODA (4.0048 g, 0.0200 mol), NTDA (5.3636 g, 0.0200 mol) and DMAP (0.1220 g, 0.0010 mol) reacted in 28.1052 g of DMSO for 4 h with nitrogen protection at 60 °C to give rise to $_6$-PAA solution with a viscosity of 0.4 dL/g. The template viscous 20 wt% PAA solution ($_5$-PAA, 3.0 dL/g) was prepared according to previous report by reaction of equal molar ODA and BPDA at 0 °C for 12 h in DMAc.[50] PVP solution (10 wt%) was prepared by dissolving PVP in DMAc. After that, the blend PAA solutions were prepared by mixing the above two solutions with $_6$-PAA/$_5$-PAA weight ratio of 90/10, 85/15, 80/20, and 70/30, respectively. The $_6$-PAA/PVP blend solutions were prepared by mixing $_6$-PAA solution and PVP solution with weight ratios of 90/10 and 80/20, respectively. The final concentration of $_6$-PAA/$_5$-PAA and $_6$-PAA/PVP solutions were diluted to 18 wt% and 16 wt% by DMAc for electrospinning. The electrospinning was performed by applying a voltage of 15 kV, a collecting distance of 25 cm, a flow rate of 1.20 mL/h, and a humidity of 23%–30%. The obtained electrospun nanofibrous membranes were then dried in a vacuum oven at 80 °C for 6 h to remove the residual solvents. After that, all the samples were treated under vacuum with the following protocol: (1) heating up to 250 °C at 5 °C/min and annealing for 30 min; (2) heating up to 370 °C at 1 °C/min and annealing for 30 min; (3) cooling down to room temperature. According to the weight ratio of $_6$-PAA, $_5$-PAA and PVP, the resultant fibrous composite membranes were marked as $_6$-PI/$_5$-PI-10, $_6$-PI/$_5$-PI-15, $_6$-PI/$_5$-PI-20, $_6$-PI/$_5$-PI-30, $_6$-PI/PVP-10, and $_6$-PI/PVP-20, respectively. In addition, to completely remove PVP, the $_6$-PAA/PVP fibrous membrane were heat treated at a final temperature of 450 °C, and the resultant sample was marked as $_6$-PI-450. To have a better comparison, neat $_5$-PI nanofibrous membranes were also fabricated by electrospinning $_5$-PAA solution followed by thermal imidization. The whole procedure for the preparation of electrospun nanofibrous membranes is shown in Fig. 1.

Hydrolysis Resistance

The chemical hydrolysis resistance (sulfuric acid, potassium hydroxide, and sodium chloride) was conducted by soaking nanofibrous membranes in 6 mol/L potassium hydroxide, 6 mol/L sulfuric acid and saturated sodium chloride at 80 °C for 6, 18, and 24 h respectively. Afterward, the samples were washed by deionized water to neutral or remove the salt, and then dried in a vacuum oven at 100 °C for 1 h. Then all these samples were characterized by morphology analysis and tensile tests.

Characterizations

The chemical structures were determined by FTIR spectra (Bruker Tensor 27). The morphologies were measured on a scanning electron microscopy (SEM, FEI Quanta 200). Dynamic

https://doi.org/10.1007/s10118-021-2634-8

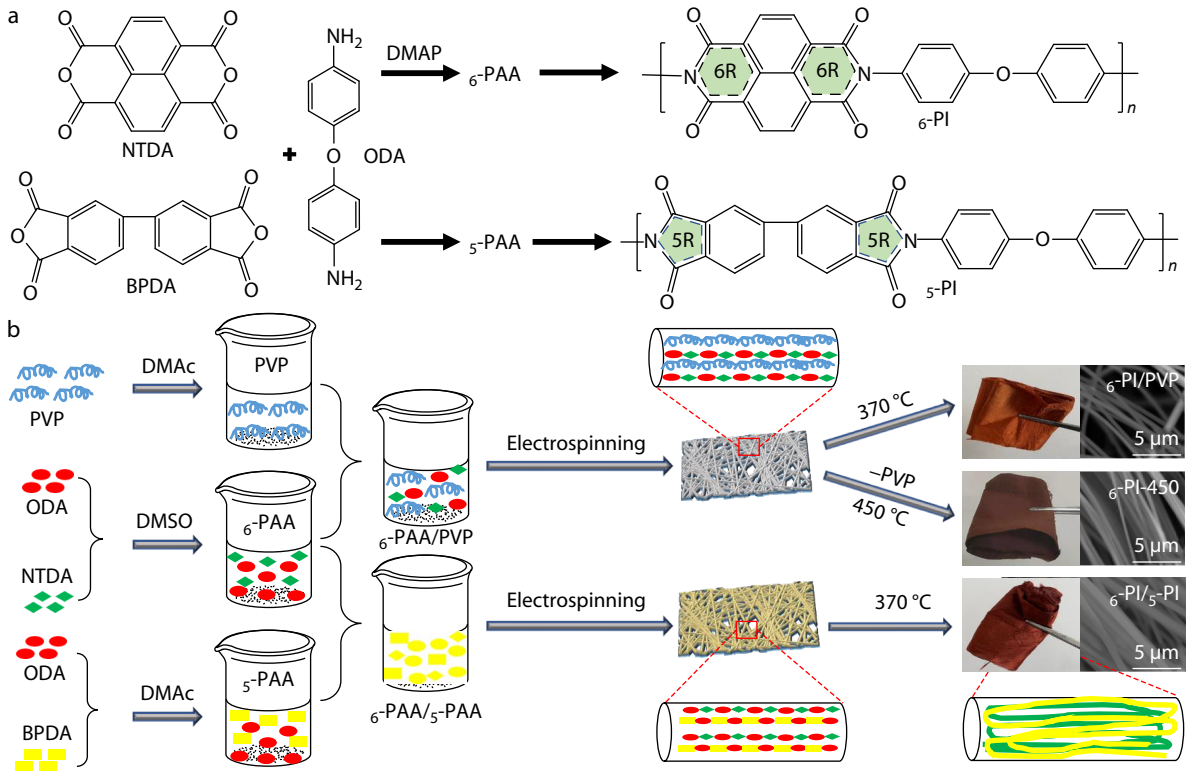

Fig. 1 Preparation of electrospun $_6$-PI, $_6$-PI/$_5$-PI and $_6$-PI/PVP nanofibers: (a) synthesis procedure of $_6$-PI and $_5$-PI polymers; (b) preparation procedure of $_6$-PI/PVP, $_6$-PI-450 and $_6$-PI/$_5$-PI nanofibrous membranes.

mechanical analysis (DMA) was performed in a PerkinElmer Diamond Analyzer which operates in the tension mode, under the temperature range from 30 °C to 500 °C at a heating rate of 3 °C/min. The mechanical properties were characterized by a universal electronic experiment machine (SANS, CMT1802) at a tensile speed of 5 mm/min. The thermal stability was measured by a thermal gravimetric analyzer (TGA, TGA55, TA) under nitrogen gas at a heating rate of 10 °C/min.

RESULTS AND DISCUSSION

Preparation of $_6$-PI Electrospun Fibrous Membranes

In this work, $_6$-PI electrospun fibrous membranes were prepared by a template-assisted method. At the beginning, the $_6$-PI precursor, $_6$-PAA dark brown solution, was synthesized without addition of catalyst, 4-dimethylaminopyridine (DMAP), and the resultant $_6$-PAA only shows a low intrinsic viscosity of 0.25 dL/g. In comparison, after adding DMAP into the reaction, the intrinsic viscosity of $_6$-PAA solution was significantly increased to 0.40 dL/g, suggesting a relatively higher molecular weight than that without catalyst. According to the intrinsic viscosity of poly(amic acid) in DMSO, the weight average molecular weight can be calculated from the Mark-Houwink equation of PAA.[51] The molecular weight of the $_6$-PAA solution synthesized without DMAP catalyst was 4570 g/mol. In contrast, the $_6$-PAA solution synthesized with DMAP catalyst was 8414g/mol, which was 1.84 times of the 6-PAA solution synthesized without DMAP. However, such $_6$-PAA solution with higher intrinsic viscosity was still not high enough for electrospinning to form electrospun nanofibers. Therefore, one of the electrospinnable solutions, $_5$-PAA light yellow solution was prepared from BPDA and ODA. It possessed a much higher intrinsic viscosity of 3.2 dL/g, suggesting the high molecular weight and suitable for electrospinning after diluting. In addition, PVP with high molecular weight of 1.76×10^6 was chosen as another electrospinnable polymer because of the good electrospinnability and low decomposition temperature of PVP. Therefore, as shown in Fig. 1, these two electrospinnable solutions were mixed with $_6$-PAA solution to prepare electrospinning solutions. After electrospinning, $_6$-PAA/$_5$-PAA and $_6$-PAA/PVP composite fibrous membranes were obtained. *Via* further thermal treatment at different temperatures, $_6$-PI/$_5$-PI, $_6$-PI/PVP, and neat $_6$-PI electrospun fibrous membranes were prepared. Herein, the addition of high molecular weight polymer solutions as electrospinning-assistance solution can guarantee the high quality nanofibrous membranes with smooth fiber surface and uniform fiber diameters.

FTIR Analysis

FTIR is an efficient technique to analyze the chemical structures. Fig. 2 presented the FTIR spectra of $_6$-PI-450, $_6$-PI/$_5$-PI and $_6$-PI/PVP fiber membranes. $_6$-PI-450 was derived from the thermal treatment of $_6$-PI/PVP-10 at 450 °C. After the thermal treatment, the PVP component was decomposed completely, only remaining very few residual char.[51] Therefore, it is difficult to observe the infrared signal from sample $_6$-PI-450 and the infrared spectrum of $_6$-PI-450 sample can be considered as the infrared absorption signal of neat $_6$-PI. Both $_6$-PI and $_5$-PI exhibit the same vibration absorption band of aromatic ring at 1500 cm^{-1}. The symmetric stretching vibration band of C=O

in six-membered imide ring appears at 1715 cm^{-1}, while asymmetric stretching vibration band appears at 1675 cm^{-1}. As comparison, the corresponding absorption bands of C=O in $_5$-PI five-membered imide ring appear at 1775 and 1710 cm^{-1}, respectively (Fig. 2, $_5$-PI-370). Similarly, the stretching vibration bands of C—N in $_6$-PI-450 and $_5$-PI-370 are also different, where 1346 and 1368 cm^{-1} are observed respectively. The above different locations for the same group in $_6$-PI and $_5$-PI could be due to the smaller tension of six-membered ring and smaller polarity of carbonyl imide and carbon-nitrogen bond in $_6$-PI than that in $_5$-PI. In addition, because of the larger conjugation group, $_6$-PI shows a stretching absorption at 1246 cm^{-1}, larger than $_5$-PI (1236 cm^{-1}). Because of the low content of PVP and $_5$-PI, $_6$-PI-450, $_6$-PI/$_5$-PI-10 and $_6$-PI/PVP-10 exhibited nearly the same spectra. The absorptions at 2955 and 2920 cm^{-1} of $_6$-PI/PVP-10 could be attributed to the vibration of C—H in aliphatic chain of PVP, because the PVP is thermally stable even at the 370 °C imidization temperature.

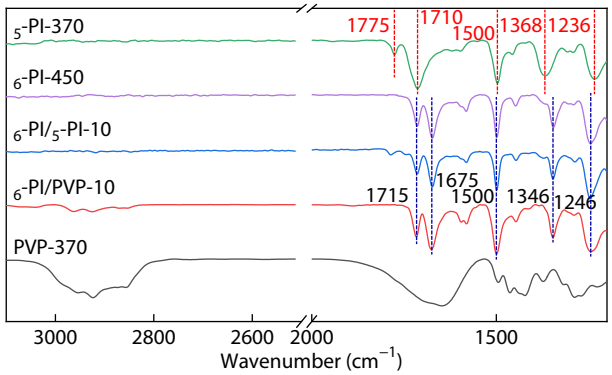

Fig. 2 FTIR spectra of $_6$-PI-450°C, $_6$-PI/$_5$-PI and $_6$-PI/PVP fiber membranes.

Thermal Properties

Thermal resistance is one of the most outstanding characteristics of PI materials. The PIs with six-membered imide ring possess much more stable structure, therefore, exhibiting better thermal resistance. Fig. 3 shows the TGA and DMA curves of $_6$-PI, $_6$-PI/$_5$-PI and $_6$-PI/PVP nanofibrous membranes and the corresponding thermal properties are summarized in Table 1. Neat $_6$-PI nanofibrous membranes ($_6$-PI-450) possess the highest thermal decomposition temperature with $T_{5\%}$ of 564 °C and $T_{10\%}$ of 579 °C. The $T_{5\%}$ and $T_{10\%}$ of $_6$-PI/$_5$-PI-30 (including 30% $_5$-PI) were 528 and 545 °C, 36 and 34 °C lower than those of $_6$-PI-450. The poorest thermal resistance was observed from $_6$-PI/PVP-20 fiber membranes, because of the low thermal resistance component of PVP (20 wt%). DMA curves (Fig. 3b) showed that the glass transition temperature (T_g) of composite nanofibrous membranes decreased with the increase of $_5$-PI or PVP content. In addition, all composite membranes exhibit only one glass transition peak between 280 and 311 °C, indicating the excellent thermal resistant of PIs and the good compatibility between $_6$-PI, $_5$-PI and PVP. However, T_g of $_6$-PI was only 306 °C, lower than expected, which could be due to the small ratio of loss modulus to storage modulus (tanδ) as well as the wide and flat peak. Therefore, it is difficult to determine the real T_g of $_6$-PI from DMA.

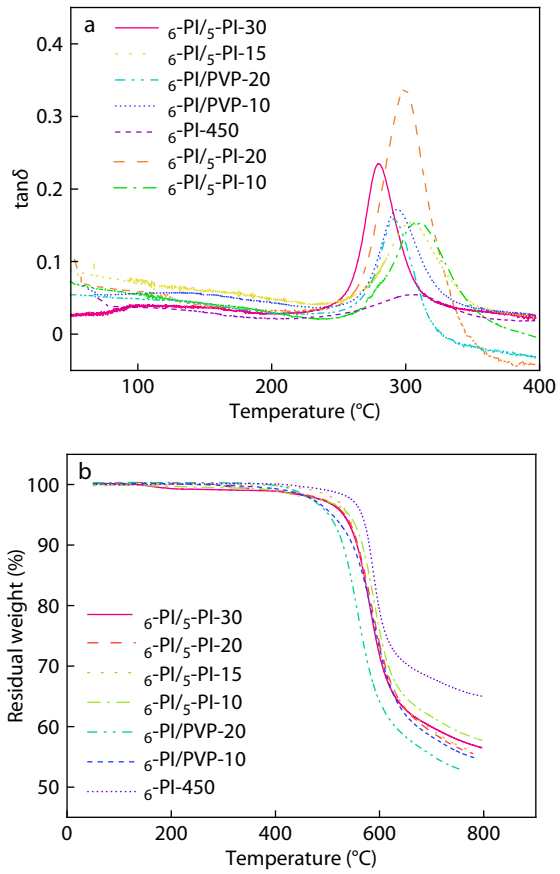

Fig. 3 TGA (a) and DMA (b) curves of $_6$-PI, $_6$-PI/$_5$-PI and $_6$-PI/PVP.

Table 1 Thermal performance data of the fibrous membrane.

Sample	$T_{5\%}$ (°C)	$T_{10\%}$ (°C)	tanδ	T_g (°C)
$_6$-PI/$_5$-PI-30	528	545	0.2349	280
$_6$-PI/$_5$-PI-20	531	553	0.1705	300
$_6$-PI/$_5$-PI-15	536	558	0.1543	304
$_6$-PI/$_5$-PI-10	539	566	0.3368	311
$_6$-PI/PVP-20	500	530	0.1523	292
$_6$-PI/PVP-10	507	546	0.1719	294
$_6$-PI -450	564	579	0.0544	306

Mechanical Properties

The obtained fibers of $_6$-PI, $_6$-PI/$_5$-PI, and $_6$-PI/PVP nanofibrous membranes presented smooth surface without obvious defects. All the fibers show the fiber diameters in the range of 0.8–1.2 μm (Fig. 4). However, these fiber membranes presented quite different mechanical properties. As shown in Fig. 5, $_6$-PI/$_5$-PI demonstrates higher tensile strength and elongation at break than those of $_6$-PI and $_6$-PI/PVP, while the mechanical property of $_6$-PI/$_5$-PI is enhanced with the increase of $_5$-PI content. $_5$-PI, as a conventional PI, possessed superior mechanical performance due to their relatively high molecular weight.[52] Similar results were also observed in $_6$-PI/PVP composite nanofibrous membranes because of the super high molecular weight of PVP.

The detailed mechanical properties of $_6$-PI, $_6$-PI/$_5$-PI and $_6$-PI/PVP are summarized in Table 2, which clearly revealed

https://doi.org/10.1007/s10118-021-2634-8

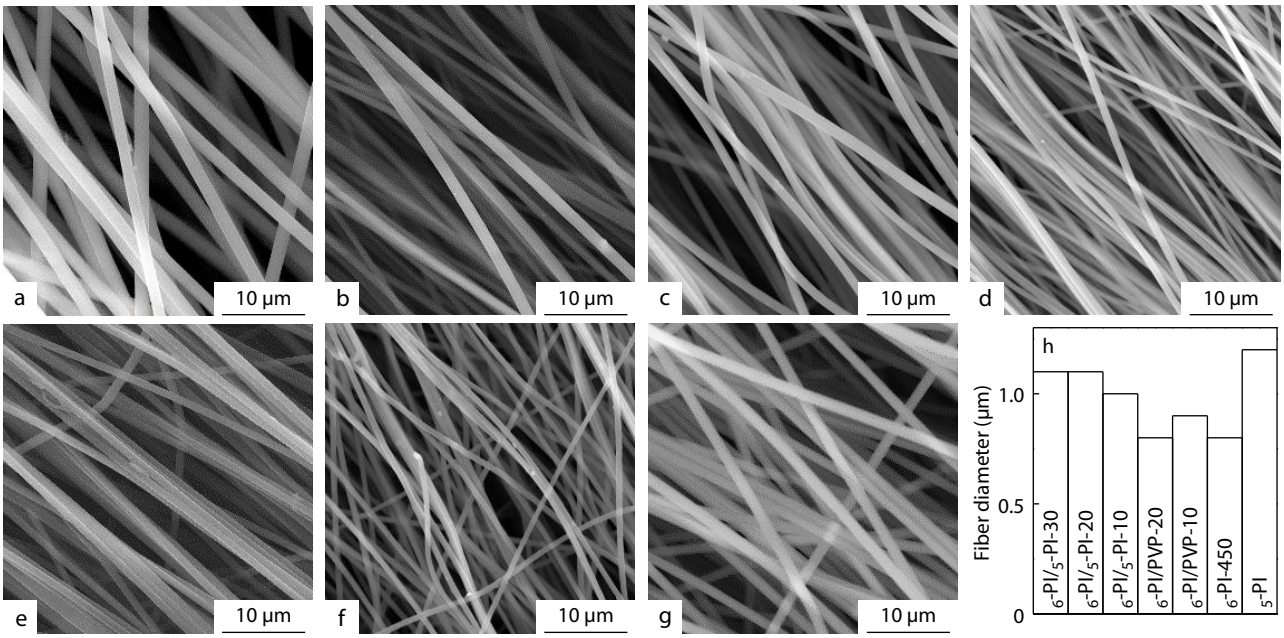

Fig. 4 SEM images of electrospun fiber membranes: (a) $_6$-PI/$_5$-PI-30; (b) $_6$-PI/5-PI-20; (c) $_6$-PI/5-PI-10; (d) $_6$-PI/PVP-20; (e) $_6$-PI/PVP-10; (f) $_6$-PI-450; (g) $_5$-PI; (h) fiber diameters of above samples.

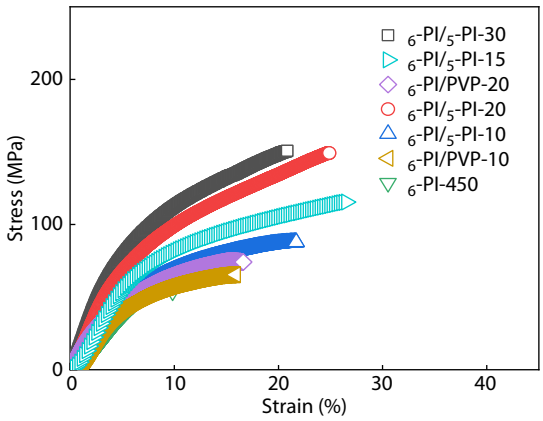

Fig. 5 Typical stress-strain curves of $_6$-PI/$_5$-PI, $_6$-PI/PVP and $_6$-PI-450 fiber membranes.

Table 2 Mechanical properties of $_6$-PI/$_5$-PI, $_6$-PI/PVP and $_6$-PI-450 fiber membranes.

Sample	Strength (MPa)	Elongation at break (%)	Modulus (GPa)
$_6$-PI/$_5$-PI-30	151±20	20.9±2.3	2.00±0.31
$_6$-PI/$_5$-PI-20	149±9	24.9±1.1	1.74±0.24
$_6$-PI/$_5$-PI-15	116±11	26.5±1.9	1.36±0.32
$_6$-PI/$_5$-PI-10	88±7	21.7±0.5	1.23±0.17
$_6$-PI/PVP-20	75±9	16.1±1.1	1.21±0.24
$_6$-PI/PVP-10	65±8	16.2±1.4	1.10±0.18
$_6$-PI -450°C	60±6	9.5±1.2	0.91±0.10

mechanical differences among these membranes. As shown in Table 2, all the membrane samples possess tensile strength, modulus, elongation at break in the range of 60–151 MPa, 0.91–2.00 GPa, and 9.5%–26.5%, respectively. In detail, $_6$-PI/PVP-10 fiber membrane with 10 wt% PVP showed tensile strength of 65 MPa, modulus of 1.1 GPa and elongation at break of 16.2%. Accordingly, $_6$-PI/$_5$-PI-10 fiber membrane with 10 wt% $_5$-PAA possessed tensile strength of 88 MPa, modulus of 1.23 GPa and elongation at break of 21.7%. In general, $_5$-PI fiber membrane should have better mechanical properties than $_6$-PI fiber membrane because of the higher molecular weight of $_5$-PI. But neat $_6$-PI membrane can be achieved by removing PVP at a high temperature above 420 °C.[53] Therefore, the neat $_6$-PI nanofibrous membranes, $_6$-PI-450, by 450 °C annealing presented much poorer mechanical performance with tensile strength of 60 MPa, modulus of 0.92 GPa and elongation at break of 9.5% than $_6$-PI/PVP-10 fiber membrane, which could be attributed to the low molecular weight of $_6$-PI.

Acid, Alkali and Salt Resistance

Alkali resistance

Although PI possess high thermal resistance and excellent mechanical properties, many imide rings exist in their molecular chains, where the carbonyl groups are sensible to water and easily hydrolyzed to shorter molecular chains, especially in alkaline conditions. For instance, the commercial PI membrane, Kapton, are facile to be decomposed in a boiling alkaline hydrazine condition to generate monomers.[54] In this work, because of the high specific surface areas and the porous structures, electrospun $_6$-PI, $_5$-PI, $_6$-PI/$_5$-PI-10, and $_6$-PI/PVP-10 nanofibrous membranes are more prone to hydrolysis and degradation. To observe the results apparently, the fiber membrane samples were stored in hot concentrated alkali solution (80 °C, 6 mol/L) for different time. After that, all the samples were observed by naked eyes and SEM images, and also characterized by tensile tests. Fig. 6(a) illustrates the photos of $_6$-PI samples after hydrolyzing at 80 °C for 6, 8 and 24 h, respectively. The appearance of samples hardly changed except a slight yellow color of alkaline solution. After immersing $_6$-PI/$_5$-PI-10 and $_6$-PI/PVP-10 fiber membranes in alkaline at 80 °C for

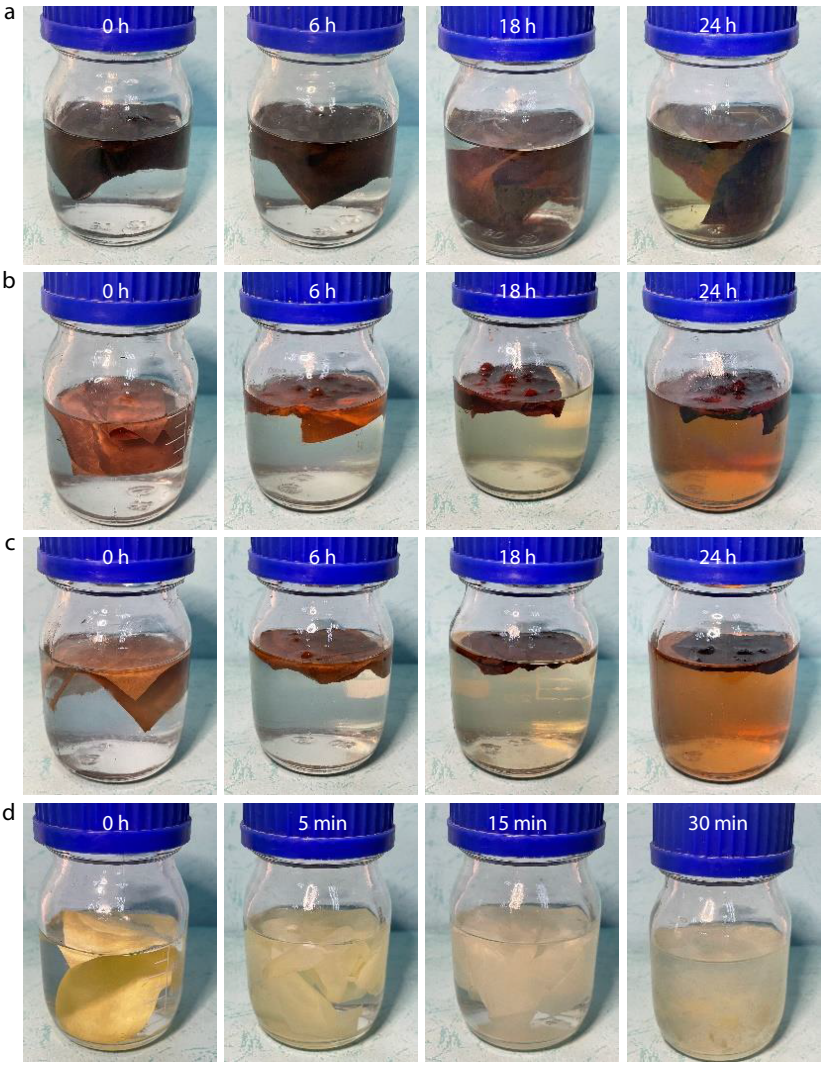

Fig. 6 Photos of different fiber membranes after alkaline treatment at 80 °C for different time. (a) $_6$-PI-450; (b) $_6$-PI/$_5$-PI-10; (c) $_6$-PI/PVP-10; and (d) $_5$-PI.

6–24 h, the color of solution was darker while nanofibrous membranes were still unbroken but seem to be softer (Figs. 6b and 6c). On the contrast, the color of traditional $_5$-PI fiber membranes transformed from golden yellow to light yellow after 5 min in alkaline solution at 80 °C. Then it changed to white after 15 min and broke into fragments after 30 min (Fig. 6d). These observations demonstrated the poor alkaline hydrolysis resistance of electrospun $_5$-PI fiber porous membranes because the five-membered imide groups could be easily attacked by OH^-, leading to the breakage of molecular chains. In contrast, in spite of small fiber diameters with large specific surface area and high contact area to alkali, electrospun $_6$-PI fiber membranes exhibited excellent hydrolysis resistance to alkaline conditions. This excellent alkaline hydrolysis resistance of $_6$-PI membrane could be attributed to the more stable six-membered ring structure of $_6$-PI molecules, avoiding the attack from OH^- of great nucleophilicity.

Further SEM characterization was used to observe the corrosion of fiber surfaces after treatment by hot alkaline for different time. As shown in Figs. 7(a) and 7(b), the fibers of both $_6$-PI-450 (24 h) and $_6$-PI/PVP-10 (6 h) are smooth without any corrosion evidence on the surfaces. However, corrosion and adhesion of fibers can be observed on sample $_6$-PI/$_5$-PI-10 fiber membranes after alkaline treatment for 6 h and 8 h (Figs. 7c and 7d), which could be because of the hydrolysis and degradation of $_5$-PI in the composite fibers. As expected, the worst alkaline resistance can be observed from sample $_5$-PI fiber membrane. Only 5 min treatment in alkaline, the fibers exhibit serious adhesion (Fig. 7e) while after 30 min treatment, all the fibers were hardly observed the fibrous morphology (Fig. 7f). All the SEM observations suggested that the alkaline resistant of PI fiber membranes with five-membered imide ring were much worse than that of the PI fiber membranes with six-membered imide ring.

Further mechanical properties were characterized to evaluate the alkaline resistance of the $_6$-PI/$_5$-PI-10, $_6$-PI/PVP-10, $_6$-PI-450 and $_5$-PI electrospun fiber membranes before and after alkaline treatment for different time. The typical stress-strain

https://doi.org/10.1007/s10118-021-2634-8

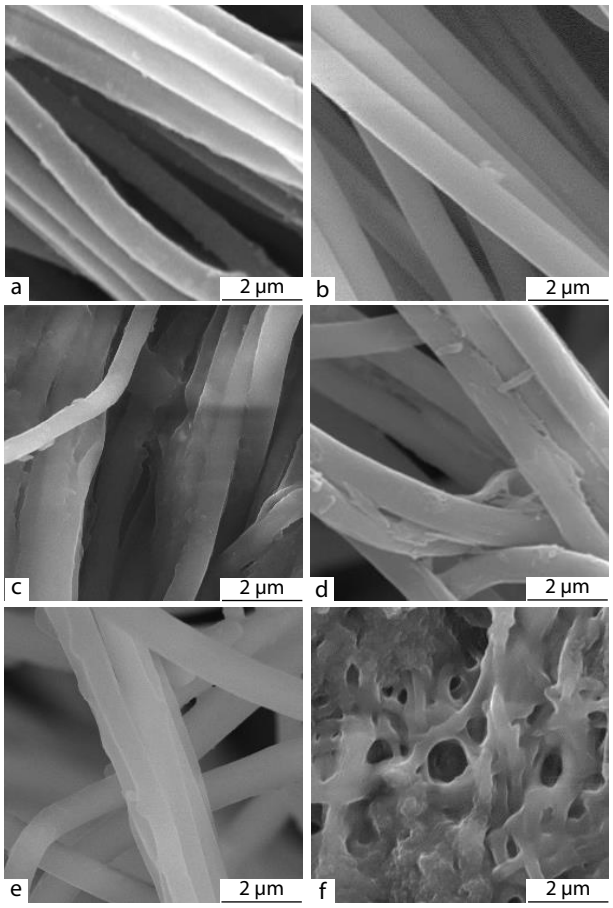

Fig. 7 SEM images of fiber membrane surface after alkaline treatment. (a) $_6$-PI-24h; (b) $_6$-PI/PVP-10-6h; (c) $_6$-PI/$_5$-PI-10-6h; (d) $_6$-PI/$_5$-PI-10-18h; (e) $_5$-PI-5 min; (f) $_5$-PI-30min.

curves are presented in Fig. 8 and the corresponding detailed mechanical properties are summarized in Table 3. In general, all the membranes showed a decrease of tensile strength and a trend of increase and decrease for elongation at break as the alkaline treatment time increased. The decrease of tensile strength could be due to the molecular degradation with alkaline treatment. The trend of elongation could be because of the slipping between the fibers from the decrease of fiber adhesion. In addition, the reduction rate of tensile strength accelerated with the increasing amount of $_5$-PI or PVP. Among all the membrane samples, $_6$-PI/$_5$-PI-30-0h membrane possessed the best tensile strength up to 150 MPa because of the high amount of the $_5$-PI component (~30 wt%) with high molecular weight. $_6$-PI/$_5$-PI-30-1h membrane showed the highest elongation at break of 59.2%, 1.5 times of that of $_6$-PI/$_5$-PI-30-0h. Such high elongation at break could be due to the remove of $_5$-PI component, leading to the decrease of adhesive force, and therefore the fibers became loose and slipped. However, because of the same reason, the tensile strength decreased dramatically to 82.2 MPa with a reduction of 45.5%. As expected, neat $_6$-PI fiber membrane, $_6$-PI-450, exhibited the best alkaline resistance with the smallest loss of tensile strength of 14.3%, 20.6%, 41.3% for alkaline treatment time of 6 h, 18 h, 24 h, respectively. While the elongation at break of $_6$-PI-450 membrane after alkaline treatment was more than

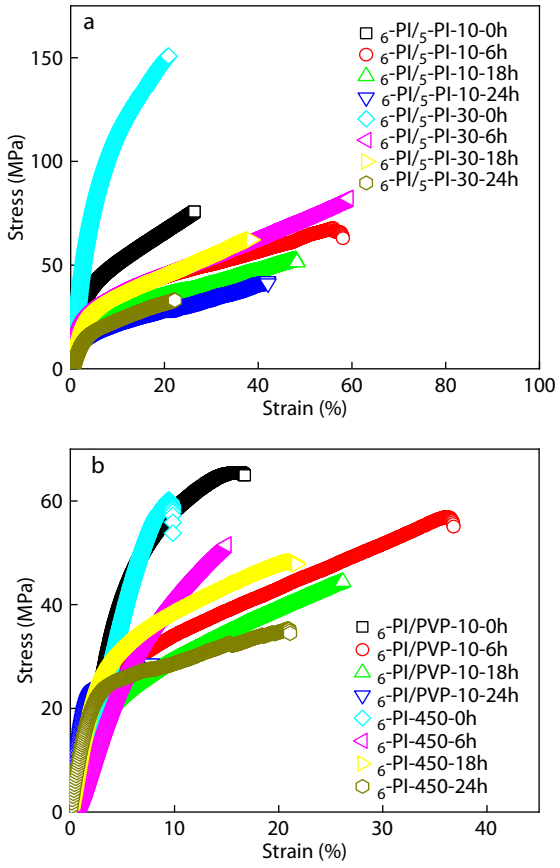

Fig. 8 Typical stress-strain curves of (a) $_6$-PI/$_5$-PI, and (b) $_6$-PI/PVP and $_6$-PI-450 after alkaline treatment for different time.

Table 3 Mechanical properties of $_6$-PI/$_5$-PI, $_6$-PI/PVP, $_6$-PI-450 and $_5$-PI after alkaline treatment for different time.

Polymer	Time	Elongation at break (%)	Strength (MPa)	Loss of strength (%)
$_6$-PI/$_5$-PI-10	0 h	26.4±0.8	75.8±5.2	0
	6 h	58.1±2.0	63.0±6.5	16.9
	18 h	48.2±5.7	52.3±5.2	30.9
	24 h	42.1±1.3	41.1±4.7	45.7
$_6$-PI/PVP-10	0 h	16.2±4.9	65.4±8.4	0
	6 h	35.9±2.6	56.8±6.5	13.1
	18 h	26.1±2.2	44.4±5.7	32.2
	24 h	7.8±3.7	28.6±3.8	56.2
$_6$-PI/$_5$-PI-30	0 h	20.8±2.3	150.7±20.3	0
	1 h	59.2±3.4	82.2±9.2	45.5
	3 h	38.5±4.1	62.2±13.6	58.7
	6 h	22.2±1.6	33.2±11.7	78.0
$_6$-PI-450	0 h	9.5±3.4	60.1±6.3	0
	6 h	14.9±1.7	51.5±7.9	14.3
	18 h	21.7±2.1	47.8±6.1	20.6
	24 h	20.9±3.2	35.3±4.4	41.3
$_5$-PI	0 h	13.9±3.5	144.0±10.2	0
	5 min	16.1±5.8	84.0±14.2	41.7
	15 min	31.1±4.2	7.1±5.1	95.1
	30 min	–	–	–

twice of the original $_6$-PI-450 membrane, and also much larger than other membrane samples after 24 h alkaline treatment. These results further demonstrated that $_6$-PI mem-

https://doi.org/10.1007/s10118-021-2634-8

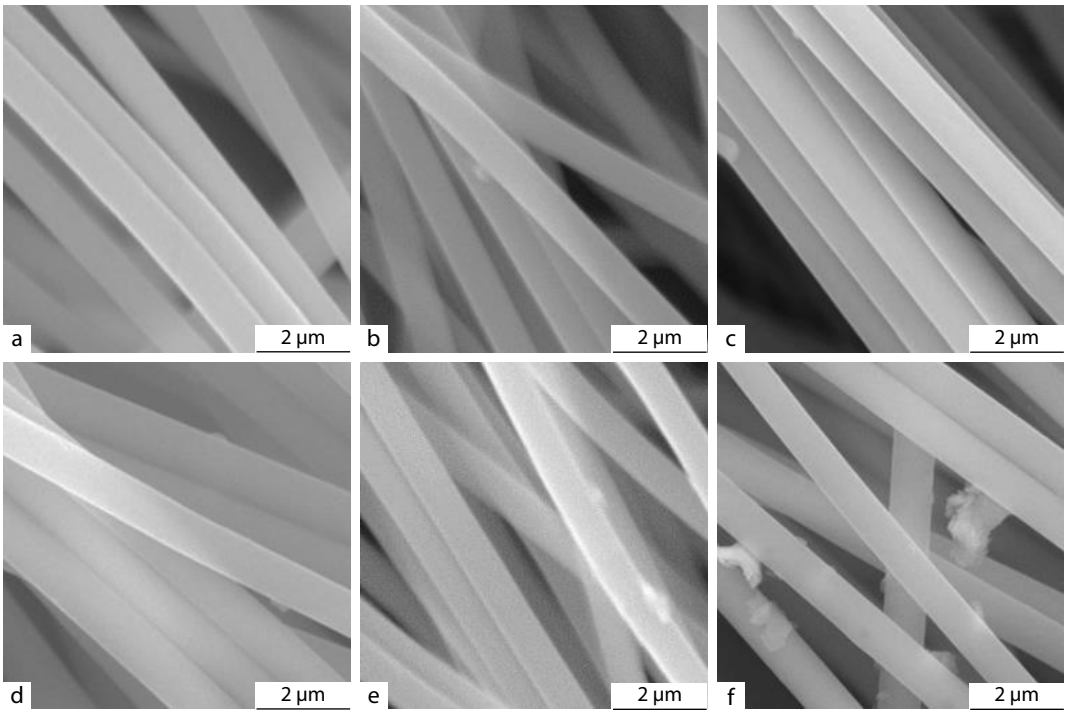

Fig. 9 SEM images of fiber membrane samples by acid (a-c) and salt (d-f) treatment. (a) $_6$-PI/$_5$-PI-10-24h; (b) $_6$-PI/PVP-10-24h; (c) $_5$-PI-24h; (d) $_6$-PI/$_5$-PI-10-24h; (e) $_6$-PI/PVP-10-24h and (f) $_5$-PI-24h.

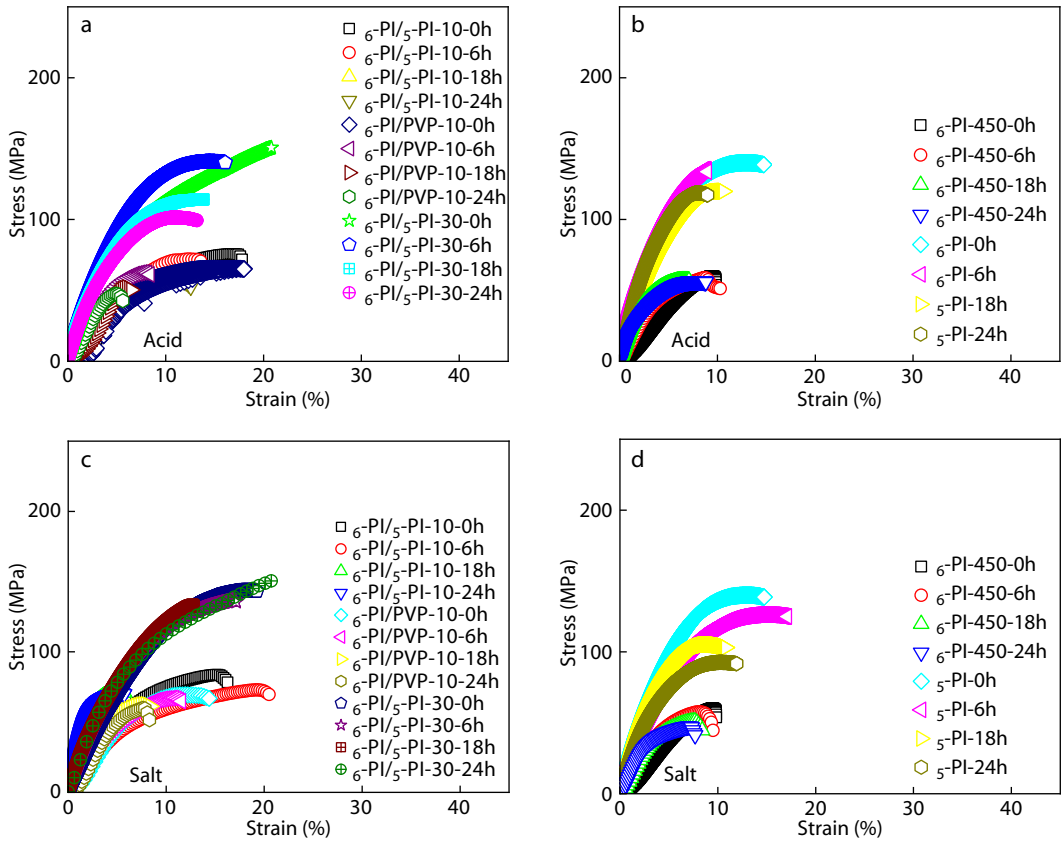

Fig. 10 Typical stress-strain curves of fiber membrane samples with acid (a, b) and salt solution (c, d) for different time.

https://doi.org/10.1007/s10118-021-2634-8

branes are the best PI materials to the alkaline resistance.

Acid and salt resistance

To evaluate the acid and salt resistance, similar treatments on the $_6$-PI/$_5$-PI, $_6$-PI/PVP, and $_5$-PI fiber membranes for different time were performed by 6 mol/L sulfuric acid and saturated sodium chloride solutions. As shown in Fig. 9, after the treatment even for 24 h, no obvious surface changes of damages were observed for all the fibers, suggesting the much better resistance to acid and salt than to alkali.

Further mechanical performance of the fiber membranes after the acid and salt treatment was evaluated by tensile tests as shown in Fig. 10 and the corresponding properties are summarized in Table 4. With the increasing treatment time in acid and salt, the mechanical performances, including tensile strength and elongation at break of all the fiber membranes became poor. However, the reduction rate was smaller in acid or salt than that in alkaline solutions while the smallest reduction rate could be obtained in salt solutions. In detail, after treatment in acid for 24 h, $_6$-PI/$_5$-PI-10 and $_5$-PI fiber membranes still exhibited a strength retention of 75%/64%, and elongation retention of 66%/64%, respectively. This suggested that PI membranes have a much better resistance to acid than to alkali, especially the $_6$-PI membrane. In addition, all the PI membranes have a relatively excellent salt resistance. After salt treatment for 24 h, the $_6$-PI/$_5$-PI-10 membrane still possessed a high tensile retention of >93%, even the neat $_5$-PI membrane still remained 81% of original strength of the untreated $_5$-PI sample. Notably, all the fiber membranes showed a significant decrease on elongation with no more than 65% retention after acid, alkali and salt treatment at 80 °C for 24 h, which could be due to the shortened molecular chains from the breakage of the PI molecules.

Table 4 Mechanical properties of $_6$-PI/$_5$-PI-10, $_6$-PI/PVP-10 and $_5$-PI after acid and salt treatment for different time.

Treatment	Polymer	Time	Elongation at break (%)	Strength (MPa)	Loss of strength (%)
Acid	$_6$-PI/$_5$-PI-10	0 h	17.1±3.8	75.6±5.6	0.0
		6 h	12.1±2.7	71.7±3.0	5.1
		18 h	10.4±4.2	62.6±5.2	17.2
		24 h	11.2±3.3	56.6±7.6	25.1
	$_6$-PI/PVP-10	0 h	16.2±4.9	65.4±8.4	0.0
		6 h	7.9±2.8	62.6±7.1	4.6
		18 h	6.0±1.5	52.3±4.3	20.0
		24 h	5.0±1.6	47.3±5.3	27.7
	$_6$-PI/$_5$-PI-30	0 h	20.8±2.3	150.7±20.3	0.0
		6 h	16.1±3.6	140.6±13.2	6.7
		18 h	13.9±1.8	114.5±8.4	24.0
		24 h	11.0±2.2	101.8±12.1	32.7
	$_6$-PI-450	0 h	9.5±3.4	60.1±6.2	0.0
		6 h	8.0±2.3	57.7±5.6	4.0
		18 h	7.5±4.2	51.2±4.3	14.9
		24 h	7.1±3.9	47.5±7.4	20.9
	$_5$-PI	0 h	13.9±3.5	144.0±10.2	0.0
		6 h	14.8±2.2	126.3±10.6	12.5
		18 h	9.2±1.8	105.7±5.4	27.1
		24 h	9.5±2.4	92.1±7.2	36.1
Salt	$_6$-PI/$_5$-PI-10	0 h	17.0±3.8	75.7±5.6	0.0
		6 h	19.3±5.2	72.9±3.2	3.7
		18 h	6.1±2.3	72.1±6.1	4.8
		24 h	5.4±3.3	70.7±2.2	6.5
	$_6$-PI/PVP-10	0 h	11.9±2.3	69.5±3.9	0.0
		6 h	10.8±2.1	67.5±2.3	2.9
		18 h	7.9±1.5	62.5±5.2	10.1
		24 h	7. 6±1.8	59.4±4.1	14.5
	$_6$-PI/$_5$-PI-30	0 h	20.8±2.3	150.7±20.3	0.0
		6 h	18.6±3.4	143.7±7.0	4.7
		18 h	16.9±2.5	136.6±11.1	9.3
		24 h	12.4±3.3	133.5±9.5	11.4
	$_6$-PI-450	0 h	9.5±3.4	60.1±6.2	0.0
		6 h	8.7±2.7	58.9±3.7	2.0
		18 h	6.8±3.4	57.1±4.8	5.0
		24 h	7.5±3.2	56.4±3.9	6.1
	$_5$-PI	0 h	13.9±3.5	144.0±10.3	0.0
		6 h	8.6±2.3	135.1±4.62	6.1
		18 h	10.4±1.2	119.4±8.5	17.1
		24 h	8.9±1.7	117.0±10.1	18.7

CONCLUSIONS

In summary, electrospun polynaphthalimide (PNI) with six-membered imide rings ($_6$-PI) nanofibrous membranes has been successfully prepared *via* a template strategy using $_5$-PI and PVP as template. The resultant neat fibrous membranes and composite membranes possessed remarkable thermal stability with $T_{5\%}$>500 °C, especially the neat $_6$-PI nanofibrous membrane with $T_{5\%}$>560 °C. The addition of template polymers can significantly improve the mechanical properties of composite nanofibrous membranes, $_6$-PI/$_5$-PI and $_6$-PI/PVP. Because the six-membered imide ring structure possesses smaller bond angle tension and higher structural stability than that with five-membered imide ring, the PNI electrospun nanofibrous membranes ($_6$-PI-450) have the best chemical resistance to strong acid, strong alkali and concentrated salt. After being treated in these chemical solutions at 80 °C for 24 h, the $_6$-PI nanofibrous membranes can still possess the smooth fiber morphology, and maintain over 50% mechanical performance of the sample without chemical treatment. Such high performance $_6$-PI electrospun nanofibrous membranes could be good candidates for applications in different chemically harsh environments.

ACKNOWLEDGMENTS

This work was financially supported by the National Natural Science Foundation of China (Nos. 21975111, 21774053, and 51803093), Natural Science Foundation of Jiangsu Province (No. BK20180770) and Open Project of Chemistry Department of Qingdao University of Science and Technology (No. QUSTHX201921).

REFERENCES

1 Xue, J.; Wu, T.; Dai, Y.; Xia, Y. Electrospinning and electrospun nanofibers: methods, materials, and applications. *Chem. Rev.* **2019**, *119*, 5298–5415.
2 Yang, X.; Wang, J.; Guo, H.; Liu, L.; Xu, W.; Duan, G. Structural design toward functional materials by electrospinning: a review. *e-Polymer* **2020**, *20*, 682–712.
3 Agarwal, S.; Greiner, A.; Wendorff, J. H. Functional materials by electrospinning of polymers. *Prog. Polym. Sci.* **2013**, *38*, 963–991.
4 Wang Z.; Xu K.; Zhang Y.; Wu J.; Lin X; Liu C.; Hua J. Study on

electro-spin performance of different types of cellulose by activation in the solvent of LiCl/DMAc. *J. For. Eng.* **2020**, *5*, 108–113.
5 Duan, G.; Jin, M.; Wang, F.; Greiner, A.; Agarwal, S.; Jiang, S. Core effect on mechanical properties of one dimensional electrospun core-sheath composite fibers. *Compos. Commun.* **2021**, *25*, 100773.
6 Xue, W.; Xu, M.; Yu, M. N.; Sun, H. M.; Lin, J. Y.; Jiang, R. C.; Xie, L. H.; Shi, N. E.; Huang, W. Electrospun supramolecular hybrid microfibers from conjugated polymers: color transformation and conductivity evolution. *Chinese J. Polym. Sci.* **2021**, *39*, 824–830.
7 Guo, H.; Chen, Y.; Li, Y.; Zhou, W.; Xu, W.; Pang, L.; Fan, X.; Jiang, S. Electrospun fibrous materials and their applications for electromagnetic interference shielding: a review. *Compos. Part A* **2021**, *143*, 106309.
8 Chen, T.; Zhong, G. C.; Zhang, Y. T.; Zhao, L. M.; Qiu, Y. J. Bio-based and biodegradable electrospun fibers composed of poly(L-lactide) and polyamide 4. *Chinese J. Polym. Sci.* **2020**, *38*, 53–62.
9 Jiang, S.; Chen, Y.; Duan, G.; Mei, C.; Greiner, A.; Agarwal, S. Electrospun nanofiber reinforced composites: a review. *Polym. Chem.* **2018**, *9*, 2685–2720.
10 Zhang D.; Cai J.; Xu W.; Dong Q.; Li Y.; Liu G.; Wang Z. Synthesis, characterization and adsorption property of cellulose nanofiber-based hydrogels. *J. For. Eng.* **2019**, *4*, 92–98.
11 Jiang, S.; Agarwal, S.; Greiner, A. Low-density open cellular sponges as functional materials. *Angew. Chem. Int. Ed.* **2017**, *56*, 15520–15538.
12 Zhang, A.; Wang, F.; Chen, L.; Wei, X.; Xue, M.; Yang, F.; Jiang, S. 3D printing hydrogels for actuators: a review. *Chin. Chem. Lett.* **2021**, *002*.
13 Zhao, L.; Duan, G.; Zhang, G.; Yang, H.; He, S.; Jiang, S. Electrospun functional materials toward food packaging applications: a review. *Nanomaterials* **2020**, *10*, 150.
14 Liu, L.; Xu, W.; Ding, Y.; Agarwal, S.; Greiner, A.; Duan, G. A review of smart electrospun fibers toward textiles. *Compos. Commun.* **2020**, *22*, 100506.
15 Miao, X.; Lin, J.; Bian, F. Utilization of discarded crop straw to produce cellulose nanofibrils and their assemblies. *J. Bioresour. Bioprod.* **2020**, *5*, 26–36.
16 Jian, S.; Tian, Z.; Zhang, K.; Duan, G.; Yang, W.; Jiang, S. Hydrothermal synthesis of Ce-doped ZnO heterojunction supported on carbon nanofibers with high visible light photocatalytic activity. *Chem. Res. Chin. Univ.* **2021**, *37*, 565–570.
17 Zheng, C.; Zhu, S.; Lu, Y.; Mei, C.; Xu, X.; Yue, Y.; Han, J. Synthesis and characterization of cellulose nanofibers/polyacrylic acid-polyacrylamide double network electroconductive hydrogel. *J. For. Eng.* **2020**, *5*, 93–100.
18 Joseph, B.; K, S. V.; Sabu, C.; Kalarikkal, N.; Thomas, S. Cellulose nanocomposites: Fabrication and biomedical applications. *J. Bioresour. Bioprod.* **2020**, *5*, 223–237.
19 Chen, T.; Wang, C.; Cheng, J.; Zhu, W.; Chen, W. Flow characteristics and mechanism of fiber suspension with the same crowding number. *J. For. Eng.* **2020**, *5*, 84–89.
20 Wei, D. W.; Wei, H.; Gauthier, A. C.; Song, J.; Jin, Y.; Xiao, H. Superhydrophobic modification of cellulose and cotton textiles: methodologies and applications. *J. Bioresour. Bioprod.* **2020**, *5*, 1–15.
21 Zhao, P.; Soin, N.; Prashanthi, K.; Chen, J.; Dong, S.; Zhou, E.; Zhu, Z.; Narasimulu, A. A.; Montemagno, C. D.; Yu, L.; Luo, J. Emulsion electrospinning of polytetrafluoroethylene (PTFE) nanofibrous membranes for high-performance triboelectric nanogenerators. *ACS Appl. Mater. Interfaces* **2018**, *10*, 5880–5891.
22 Tang, L.; Zhang, J.; Tang, Y.; Zhou, Y.; Lin, Y.; Liu, Z.; Kong, J.; Liu, T.; Gu, J. Fluorine/adamantane modified cyanate resins with wonderful interfacial bonding strength with PBO fibers. *Compos. Part B* **2020**, *186*, 107827.
23 Xu, T.; Han, D.; Zhu, Y.; Duan, G.; Liu, K.; Hou, H. High strength electrospun single copolyacrylonitrile (coPAN) nanofibers with improved molecular orientation by drawing. *Chinese J. Polym. Sci.* **2021**, *39*, 174–180.
24 Yao, K.; Chen, J.; Li, P.; Duan, G.; Hou, H. Robust strong electrospun polyimide composite nanofibers from a ternary polyamic acid blend. *Compos. Commun.* **2019**, *15*, 92–95.
25 Duan, G.; Fang, H.; Huang, C.; Jiang, S.; Hou, H. Microstructures and mechanical properties of aligned electrospun carbon nanofibers from binary composites of polyacrylonitrile and polyamic acid. *J. Mater. Sci.* **2018**, *53*, 15096–15106.
26 Chen, L.; Xu, Z.; Wang, F.; Duan, G.; Xu, W.; Zhang, G.; Yang, H.; Liu, J.; Jiang, S. A flame-retardant and transparent wood/polyimide composite with excellent mechanical strength. *Compos. Commun.* **2020**, *20*, 100355.
27 Ye, W.; Zhu, J.; Liao, X.; Jiang, S.; Li, Y.; Fang, H.; Hou, H. Hierarchical three-dimensional micro/nano-architecture of polyaniline nanowires wrapped-on polyimide nanofibers for high performance lithium-ion battery separators. *J. Power Sources* **2015**, *299*, 417–424.
28 Yang, H.; Lee, J.; Cheong, J. Y.; Wang, Y.; Duan, G.; Hou, H.; Jiang, S.; Kim, I. D. Molecular engineering of carbonyl organic electrodes for rechargeable metal-ion batteries: fundamentals, recent advances, and challenges. *Energy Environ. Sci.* **2021**, *14*, 4228–4267.
29 Jiang, S.; Uch, B.; Agarwal, S.; Greiner, A. Ultralight, thermally insulating, compressible polyimide fiber assembled sponges. *ACS Appl. Mater. Interfaces* **2017**, *9*, 32308–32315.
30 Guo, Y.; Yang, X.; Ruan, K.; Kong, J.; Dong, M.; Zhang, J.; Gu, J.; Guo, Z. Reduced graphene oxide heterostructured silver nanoparticles significantly enhanced thermal conductivities in hot-pressed electrospun polyimide nanocomposites. *ACS Appl. Mater. Interfaces* **2019**, *11*, 25465–25473.
31 Kowsari, E.; Zare, A.; Ansari, V. Phosphoric acid-doped ionic liquid-functionalized graphene oxide/sulfonated polyimide composites as proton exchange membrane. *Int. J. Hydrogen Energy* **2015**, *40*, 13964–13978.
32 Li, C.; Li, S.; Lv, L.; Su, B.; Hu, M. Z. High solvent-resistant and integrally crosslinked polyimide-based composite membranes for organic solvent nanofiltration. *J. Membr. Sci.* **2018**, *564*, 10–21.
33 Jiang, S.; Hou, H.; Agarwal, S.; Greiner, A. Polyimide nanofibers by "green" electrospinning *via* aqueous solution for filtration applications. *ACS Sustain. Chem. Eng.* **2016**, *4*, 4797–4804.
34 Sezer Hicyilmaz, A.; Altin, Y.; Bedeloglu, A. Polyimide-coated fabrics with multifunctional properties: flame retardant, UV protective, and water proof. *J. Appl. Polym. Sci.* **2019**, *136*, 47616.
35 Stephans, L. E.; Myles, A.; Thomas, R. R. Kinetics of alkaline hydrolysis of a polyimide surface. *Langmuir* **2000**, *16*, 4706–4710.
36 Hatori, H.; Yamada, Y.; Shiraishi, M.; Yoshihara, M.; Kimura, T. The mechanism of polyimide pyrolysis in the early stage. *Carbon* **1996**, *34*, 201–208.
37 Kumagai, S.; Hosaka, T.; Kameda, T.; Yoshioka, T. Steam pyrolysis of polyimides: effects of steam on raw material recovery. *Environ. Sci. Technol.* **2015**, *49*, 13558–13565.
38 Xu, Y.; Zehnder, A. T. Moisture degradation effects on the

mechanical properties of HFPE-II-52 polyimide: experiments and modeling. *Exp. Mech.* **2017**, *57*, 857–869.
39 Kumagai, S.; Hosaka, T.; Kameda, T.; Yoshioka, T. Pyrolysis and hydrolysis behaviors during steam pyrolysis of polyimide. *J. Anal. Appl. Pyrolysis* **2016**, *120*, 75–81.
40 Tao, L.; Yang, H.; Liu, J.; Fan, L.; Yang, S. Fluorinated polybenzimidazopyrrolones with excellent alkaline-hydrolysis resistance. *J. Appl. Polym. Sci.* **2014**, *131*, 40041.
41 Meyer, G.; Perrot, C.; Gebel, G.; Gonon, L.; Morlat, S.; Gardette, J. L. *Ex situ* hydrolytic degradation of sulfonated polyimide membranes for fuel cells. *Polymer* **2006**, *47*, 5003–5011.
42 Perrot, C.; Meyer, G.; Gonon, L.; Gebel, G. Ageing mechanisms of proton exchange membrane used in fuel cell applications. *Fuel Cells* **2006**, *6*, 10–15.
43 UrRehman, S.; Li, P.; Zhou, H.; Zhao, X.; Dang, G.; Chen, C. Thermally and hydrolytically stable polyimides containing naphthalimide units. *Polym. Degrad. Stab.* **2012**, *97*, 1581–1588.
44 Pan, Z. F.; An, L.; Zhao, T. S.; Tang, Z. K. Advances and challenges in alkaline anion exchange membrane fuel cells. *Prog. Energy Combust. Sci.* **2018**, *66*, 141–175.
45 Piroux, F.; Mercier, R.; Picq, D.; Espuche, E. On the polynaphthalimide synthesis—influence of reaction conditions. *Polymer* **2004**, *45*, 6445–6452.
46 Shang, Y.; Xie, X.; Jin, H.; Guo, J.; Wang, Y.; Feng, S.; Wang, S.; Xu, J. Synthesis and characterization of novel sulfonated naphthalenic polyimides as proton conductive membrane for DMFC applications. *Eur. Polym. J.* **2006**, *42*, 2987–2993.
47 Qian, K.; Fang, J.; Liu, R.; Jiang, J.; Tong, J.; Guo, X.; Feng, J. Six-membered ring copolyimides as novel high performance membrane materials for gas separations. *Mater. Today Commun.* **2018**, *14*, 254–262.
48 Li, W.; Zhang, S.; Chen, G.; Zhang, Q. A new class of high T_g and organosoluble polynaphthalimides. *Polymer* **2007**, *48*, 3082–3089.
49 Song, Y.; Liu, C.; Ren, D.; Jing, L.; Jiang, Z.; Liu, B. Fluorinated/non-fluorinated sulfonated polynaphthalimides as proton exchange membranes. *Macromol. Res.* **2012**, *21*, 484–492.
50 Ding, Y.; Hou, H.; Zhao, Y.; Zhu, Z.; Fong, H. Electrospun polyimide nanofibers and their applications. *Prog. Polym. Sci.* **2016**, *61*, 67–103.
51 Swanson, S. A.; Cotts, P. M. ; Siemens, R.; Kim, S. H. Synthesis and solution properties of poly[*N*,*N*'-(*p*-phenylene)-3,3',4,4'-biphenyltetracarboxylic acid diamide]. *Macromolecules* **1991**, *24*, 1352–1357.
52 Chen, S.; Han, D.; Hou, H. High strength electrospun fibers. *Polym. Adv. Technol.* **2011**, *22*, 295–303.
53 Du, Y. K.; Yang, P.; Mou, Z. G.; Hua, N. P.; Jiang, L. Thermal decomposition behaviors of PVP coated on platinum nanoparticles. *J. Appl. Polym. Sci.* **2006**, *99*, 23–26.
54 Dine-Hart, R.; Parker, D.; Wright, W. J. B. P. J. Oxidative degradation of a polyimide film: II. Studies using hydrazine hydrate. *Br. Polym. J.* **1971**, *3*, 226–234.

https://doi.org/10.1007/s10118-021-2634-8